# DEMONSTRATION OF TRANSVERSE-TO-LONGITUDINAL EMITTANCE EXCHANGE AT A0 PHOTOINJECTOR *

J. Ruan[1], A. S. Johnson[1], Y.-E Sun[2], A. Lumpkin[1], R. Thurman-Keup[1]
[1] Accelerator Division, Fermi National Accelerator Laboratory, Batavia, IL 60510, USA
[2] Accelerator Physics Center, Fermi National Accelerator Laboratory, Batavia, IL 60510, USA

*Abstract*

The 3-D phase-space manipulation of electron beams enhances the performance of next generation accelerators including high energy colliders and accelerator based light sources. In this paper we will report an observation of near ideal transverse to longitudinal emittance exchange at the Fermilab A0 Photoinjector (A0PI). The emittance exchange (EEX) beamline consists a 3.9 GHz normal conducting deflecting mode cavity positioned between two magnetic doglegs. We will also compare the experimental results to simulations.

## INTRODUCTION

An ultra-low emittance electron source is critical to the further development of the next-generation light sources. Phase space manipulation techniques could play a very important role in this field. For example, an emittance exchange technique could swap a large transverse emittance with a smaller longitudinal emittance to achieve low transverse beam. There have been several proposed schemes to accomplish this, all of which are centered around a deflecting mode radio frequency (rf) cavity [1–4]. In this paper we will report on the demonstration of emittance exchange between transverse and longitudinal emittance at the A0 Photoinjector [5].

The emittance exchange (EEX) experiment can be described through linear optics as a transformation matrix, $M_{\mathrm{EEX}}$, that operates on the initial horizontal transverse emittance parameters $(x, x')$ and longitudinal emittance parameters $(z, \frac{\Delta p}{p})$, leaving the vertical transverse emitance unchanged [1–3]:

$$\begin{pmatrix} x \\ x' \\ z \\ \frac{\Delta p}{p} \end{pmatrix}_{\mathrm{out}} = \begin{pmatrix} \boldsymbol{A} & \boldsymbol{B} \\ \boldsymbol{C} & \boldsymbol{D} \end{pmatrix} \begin{pmatrix} x \\ x' \\ z \\ \frac{\Delta p}{p} \end{pmatrix}_{\mathrm{in}}, \qquad (1)$$

where $\boldsymbol{A}$, $\boldsymbol{B}$, $\boldsymbol{C}$ and $\boldsymbol{D}$ are $2 \times 2$ sub-matricies of $M_{\mathrm{EEX}}$. A perfect emittance exchange matrix will exist when the elements of the diagonal sub-blocks, $\boldsymbol{A}$ and $\boldsymbol{D}$ become zero and the $\boldsymbol{B}$ and $\boldsymbol{C}$ sub-blocks are populated. Due to the finite length of our $TM_{110}$ deflecting mode cavity, many of the on-diagonal elements are non-zero [5]. Higher-order effects such as space charge and coherent synchrotron radiation also contribute to an imperfect exhange.

* This work was supported by Fermi Research Alliance, LLC under contract No. DE-AC02-07CH11359 with the U.S. Department of Energy.

## EXPERIMENTAL SETUP

The EEX experiment is conducted at Fermilab's A0 Photoinjector [6]; see Figure 1. The three solenoid lenses that surround the gun control the beam's transverse size and emittance. The beam then enters a 1.3 GHz superconducting radio frequency booster cavity bringing the final energy to 14.3 MeV. Following this final acceleration stage are various diagnostic crosses consisting of either optical transition radiation (OTR) or cerium doped yttrium aluminum garnet (YAG:Ce) crystal viewers. Also found in the beamline are quadrupoles, dipole correctors and beam position monitors.

The emittance exchange beamline at the A0PI, shown in Figure 1, consists of a 3.9 GHz $TM_{110}$ deflecting mode cavity located between two horizontal dogleg magnetic channels. The $TM_{110}$ deflecting mode cavity is a liquid nitrogen cooled, normal conducting variant of a superconducting version previously developed at Fermilab [7, 8]. The time varying longitudinal electric field of the $TM_{110}$ mode increases linearly in the horizontal plane with the value of the electric field changing sign as it goes through zero at the central axis ($E_z \propto x$). The dispersion introduced by the first magnetic dogleg horizontally positions off-momentum electrons ($\delta \neq 0$) in the $TM_{110}$ cavity causing them to receive a negative longitudinal kick proportional to their $\delta$. As a result, the $TM_{110}$ cavity reduces the momentum spread. The time varying vertical magnetic field is 90 ° advanced of the electric field. The synchronous particle is timed to cross the cavity center at the peak of the electric field when the magnetic field is zero, and as a consequence, the cavity produces a time dependent positive (negative) horizontal kick with respect to early (late) particles. The synchronous particle is undeflected as it sees no fields. The final dogleg removes beam correlations resulting in the un-coupled exchange of horizontal and longitudinal emittances.

It is very important to set the cavity strength on the deflecting cavity so the diagonal sub-blocks $\boldsymbol{A}$ and $\boldsymbol{D}$ become zero. Experimentally we did it by doing a scan of the outgoing momentum offset versus the incoming momentum

ISBN 978-3-95450-117-5

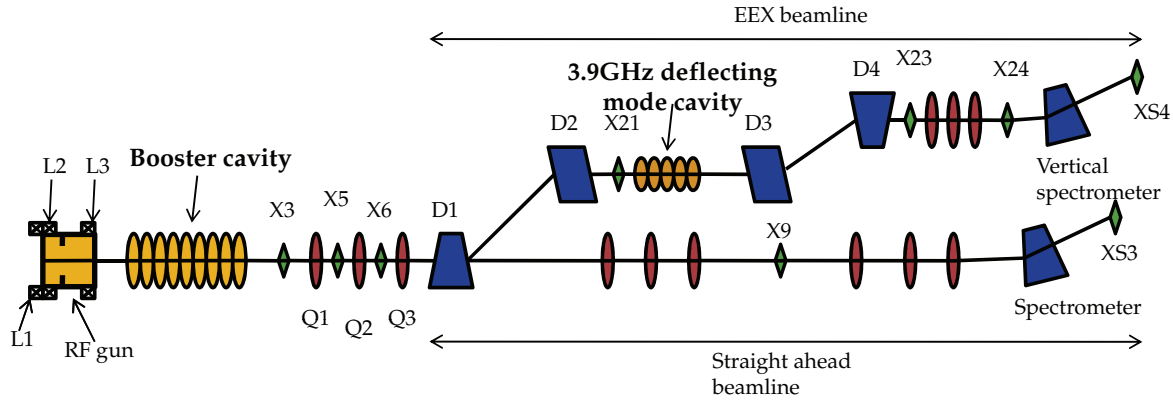


Figure 1: Top view of the A0 photoinjector showing elements pertinent to performing emittance exchange. Elements labeled "X" are diagnostics stations (beam viewers and/or multi-slit mask locations), "L" are solenoid lenses, and "Q" are quadrupole magnets.

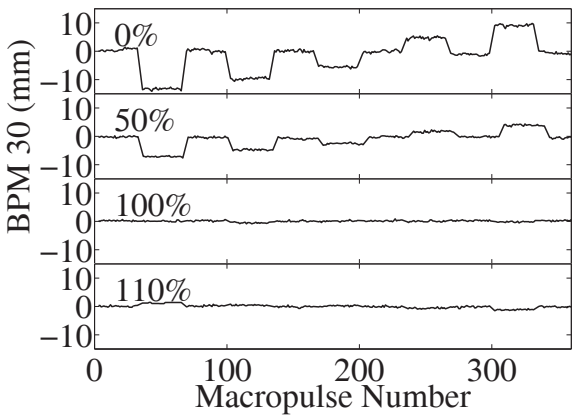


Figure 2: The first panel shows the momentum program schedule of sixty pulses at nominal momentum, followed by sixty pulses at a 2.2 percent decrease in central momentum, then sixty more samples at nominal momentum, followed by a 1.4 percent reduction, and so on. Subsequent panels show the reduction in output momentum as the $TM_{110}$ cavity strength is increased. The final panel demonstrates overcompensation by too high of a gradient.

offset. Figure 2 shows a sequence of output momenta registered by a spectrometer for four different cavity strengths. With the deflecting cavity off, any input momentum offset carries through to the output of the exchange line as shown in the top panel of figure 2. Under the exchange condition, longitudinal input parameters are converted to transverse output parameters, thus a change of the input momentum will not be seen in the output of the EEX line just as shown at the third panel of Fig. 2.

Transverse emittance measurements are made using the slit measurement technique [9]. Transverse beam profiles are measured by inserting an OTR screen at X3 and X23. Divergence measurements are made by inserting a tungsten multi-slit mask into the beam path at both X3 and X23. The masks consist of 50 $\mu$m wide slits separated by 1 mm, except at X23 where the horizontal slits are separated by 2 mm. Downstream images are generated by single crystal YAG:Ce scintillator screens oriented orthogonal to the incident beam direction. A 45 ° mirror directs the radiation to the optical system. This configuration eliminates depth-of-focus issues from the field of view [10]. A MATLAB-based program calculates the emittances and the Courant-Snyder parameters ($\alpha$,$\beta$,$\gamma$) based on the X3-X5, X3-X6 and X23-X24 spot and slit image pairs [13]. Figure 3 (a) and (b) shows a typical set of incoming horizontal beam size data and a complete set of horizontal beamlets as viewed on the X6 YAG:Ce screen. For comparison, the transverse beam profile after exchange at X23 and the beamlets as viewed at X24 are shown at Figure 3 (d) and (e). Reconstructed phase space for incoming and outgoing beam are shown at Fig. 3 (c) and (f) respectively.

Projected longitudinal emittance measurements are made by combining energy spread and bunch length measurements. EEX input and output central momenta and momentum spreads are measured by two spectrometer magnets and down-stream viewing screens. Because the longitudinal diagnostics are not capable of measuring the energy-time correlation, the booster cavity rf is tuned for a minimum energy spread, $\alpha_z = 0$. The bunch length is then determined at the X9 OTR screen using a Hamamatsu C5680 streak camera operating with a synchroscan vertical plug-in unit phase locked to 81.25 MHz as described previously [11]. The bunch length measurement at X24 is made with OTR transported to the streak camera and with the far infrared coherent transition radiation transported to a Martin-Puplett interferometer [12].

## EXPERIMENT AND SIMULATION RESULTS

The direct measurement of the emittance exchange has been performed at 14.3 MeV with a bunch charge of 250 pC, chosen as a compromise between diagnostic re-



ISBN 978-3-95450-117-5

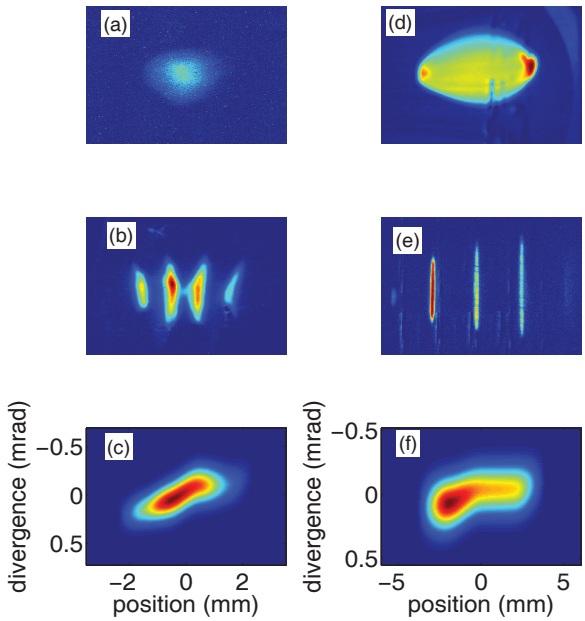


Figure 3: Horizontal emittance images for 250 pC charge before and after EEX Beamline. Beam-profile image taken at X3 OTR screen (a) and beam image taken at X6 with slits (b) before EEX beamline. Beam-profile image taken at X23 OTR screen (d) and beam image taken at X24 with slits(e) after EEX beamline. Phase space information based on the above images is plotted in (c) and (f) respectively.

quirements and space-charge effects. Transverse input Courant-Snyder parameters were tuned by adjusting Q1, Q2 and Q3. Since the intensity of the coherent transition radiation is inversely proportional to the bunch length, the interferometer's pyroelectric sensors are used to make quick, but uncalibrated, relative bunch-length measurements. This is very useful in mapping the effects of the input quadrupole fields on output longitudinal parameters. A normalized $1/\sigma_p\sigma_z$ product map is shown in Figure 4. EEX operating points were selected when the $\sigma_p\sigma_z$ product was a minimum, i.e. the bright region in Fig. 4. Input longitudinal conditions were set by operating the booster cavity for minimum energy spread as measured at XS3. Complete measurements of the initial and final emittances were collected with these conditions. The energy spread measured after EEX beamline is smaller than energy spread before EEX beamline [5]. At the same time streak camera data also indicates a dramatic decrease of the bunch length [10]. The A0PI input beam's horizontal emittance measured $\varepsilon_x^n$=2.9±0.1 mm-mrad and the EEX output longitudinal emittance measured $\varepsilon_z^n$=3.1±0.3 mm-mrad demonstrating a 1:1 transfer of $\varepsilon_{x,in}^n$ to $\varepsilon_{z,out}^n$. Similarly the input longitudinal emittance, $\varepsilon_{z,in}^n$=13.1±1.3 mm-mrad and the EEX output horizontal emittance measured $\varepsilon_{x,out}^n$=11.3±1.1 mm-mrad demonstrating a 1:1 transfer of $\varepsilon_{z,in}^n$ to $\varepsilon_{x,out}^n$. The vertical emittance was left unaffected,

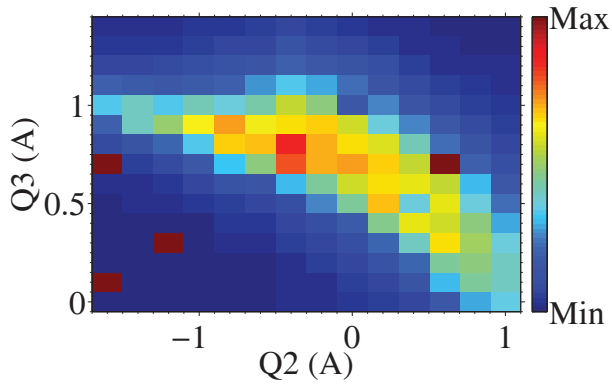


Figure 4: A relative output 1/ $\sigma_p\sigma_z$ product map against input quadrupole currents.

$\varepsilon_{y,in}^n$=2.4±0.1 mm-mrad ⇒ $\varepsilon_{y,in}^n$=2.9±0.5 mm-mrad. The combined results show the successful exchange of emittance between two planes while conserving the full 6D phase space volume.

Numerical simulations of beam dynamics through the emittance-exchange beamline are performed using General Particle Tracer (GPT) [14] with 3D space charge on and off. Initial beam parameters are matched with the experimentally measured beam parameters prior to emittance exchange including the transverse emittances and Courant-Synder parameters measured at X3, and the longitudinal beam properties measured in the straight-ahead beamline. Measured field maps of the dipole magnets and simulated deflecting cavity field maps are used. The transverse and longitudinal emittance evolutions along the EEX beamline are plotted in top and bottom of Fig. 5. A perfect emittance exchange is observed with the space-charge off, while with space-charge on, the longitudinal emittance after EEX increases in the drift following the last dipole magnet. This is due to the longitudinal space charge force induced energy spread as the bunch is compressed to less than 1 ps long after the EEX.

## FUTURE APPLICATION

As a novel phase space manipulation technique several proposals have been suggested to utilize this combined with other method such as flat beam transformation to drive the next generation light source [2, 15, 16]. Sun et al. demonstrated a novel way to generate femtosecond bunch train [17] using EEX beamline and observed coherently enhanced tunable narrow-band terahertz transition radiation from the bunch train [18]. Piot et al. also proposed a general method for tailoring the current distribution of the electron bunches [19]. Very recently Zholents and Zolotorev proposed a new type of bunch compressor with the application of this technique [20].

ISBN 978-3-95450-117-5

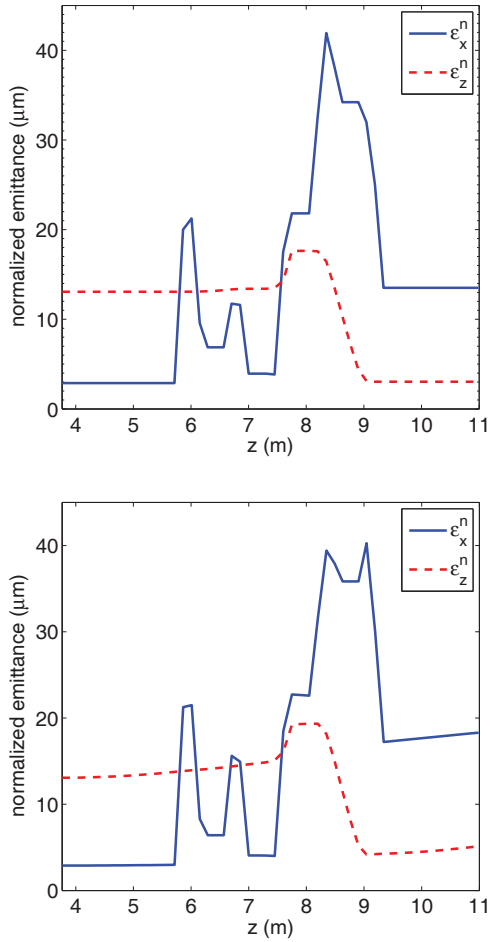


Figure 5: Simulated normalized emittance along the EEX beamline with (bottom) and without (top) 3D space charge using GPT.

## CONCLUSION

A proof-of-principle EEX experiment utilizing the Fermilab A0 Photoinjector has been completed for a beam charge of 250 pC. A 1:1 emittance exchange was observed at 14.3 MeV. The horizontal and longitudinal phase spaces were exchanged, while the vertical phase space was left unaffected.

## ACKNOWLEDGEMENT

The authors acknowledge the great effort by T. Koeth and R. Fliller for the design and setup of the EEX beamline, intitial experimental results, numerous friendly and fruitful discussions. We greatly appreciate the discussions and comments from H. Edwards, P. Piot, D. Edwards, M. Cooke. We are grateful for the support from M. Davidsaver, E. Harms, M. Cornacchia, W. Muranyi, B. Tennis, E. Lopez, R. Montiel, R. Andrews, B. Popper, J. Santucci, G. Cancelo, B. Chase, J. Branlard, P. Prieto, M. Stauffer and M. Church.

## REFERENCES

[1] M. Cornachia, and P. Emma, *Phys. Rev. ST Accel. Beams* **6** 030702 (2003).

[2] P. Emma, Z. Huang, K.-J. Kim, and P. Piot, *Phys. Rev. ST Accel. Beams* **9**, 100702 (2006).

[3] K.-J. Kim and A. Sessler, AIP Conf. Proc. **821**, 115 (2006).

[4] D.A. Edwards, private communication.

[5] J. Ruan, A. S. Johnson, A. H. Lumpkin, R. Thurman-Keup, H. Edwards , R.P. Fliller, T.W. Koeth and Y.-E Sun, *Phys. Rev. Lett* **106**, 244801 (2011).

[6] J.-P. Carneiro, *et al, Phys. Rec. ST Accel. Beams* **8**, 040101 (2005).

[7] M. McAshan and R. Wanzenberg, FNAL TM-2144, 2001.

[8] T. W. Koeth, *"An Observation of a Transverse to Longitudinal Emittance Exchange at the Fermilab A0 Photoinjector"* (Doctoral Dissertation), Rutgers University, Piscataway, NJ. (2009).

[9] C. H. Wang, *et al*, "Slits Measurement of Emittance on TTF," *International Conference on Accelerator and Large Experimental Physics Control Systems*, Trieste, Italy (1999).

[10] A. H. Lumpkin, A. S. Johnson, J. Ruan, J. Santucci, Y.-E Sun, R. Thurman-Keup, and H. Edwards, *Phys. Rev. ST Accel. Beams* **14**, 060704 (2011).

[11] A. H. Lumpkin, *et al*, "Initial Synchroscan Streak Camera Imaging at the A0 Photoinjector," *Proceedings of the 2008 Beam Instrumentation Workshop*, Lake Tahoe, CA (2008).

[12] R. M. Thurman-Keup, *et al*, "Bunch Length Measurement at the Fermilab A0 Photoinjector using a Martin-Pupplett Interferometer," *Proceedings of the 2008 Beam Instrumentation Workshop*, Lake Tahoe, CA (2008).

[13] R. M. Thurman-Keup, *et al., Proceedings of the 2011 Particle Accelerator Conference* (PAC11), New York, New York (2011)

[14] http://www.pulsar.nl/gpt/

[15] B. Carlsten, *et al., Proceedings of the Physics and Applications of High Brightness Electron Beams* (HBEB), Maui Hawaii, Nov. 2009 (unpublished).

[16] B. Jiang, J. G. Power, R. Lindberg, W. Liu, and W. Gai, *Phys. Rev. Lett* **11**, 114801 (2011).

[17] Y.-E Sun, P. Piot, A. Johnson, A. H. Lumpkin, T. J. Maxwell, J. Ruan, and R. Thurman-Keup, *Phys. Rev. Lett* **23**, 234801 (2010).

[18] P. Piot, Y.-E Sun, T. J. Maxwell, J. Ruan, A. H. Lumpkin,M. M. Rihaoui and R. Thurman-Keup, *Appl. Phys. Lett* **98**, 261501 (2010).

[19] P. Piot, Y.-E Sun, J. G. Power and M. Rihaoui, *Phys. Rev. ST Accel. Beams* **14**, 22801 (2011).

[20] A. A. Zholents and M. S. Zolotorev "A New Type of Bunch Compressor and Seeding of a Short Wave Length Coherent Radiation", Light Source, Technical Notes ANL/APS/LS-327.



ISBN 978-3-95450-117-5